HEFAT2010
7th International Conference on Heat Transfer, Fluid Mechanics and Thermodynamics
19-21 July 2010
Antalya, Turkey

EFFECT OF NOZZLE NUMBER ON CHARACTERISTICS OF MULTIPLE PLUME IN ATGM

Sung Ho Ko*, Young Kyun Kwack and Seung Yeul Han
*Author for correspondence
Department of Mechanical Design Engineering,
Chungnam National University,
220 Gung-dong, Yusung-gu, Daejeon,
Korea,
E-mail: sunghoko@cnu.ac.kr

ABSTRACT

Numerical studies were performed to analyze effect of nozzle number of antitank guided missile(ATGM) on characteristics of a plume and supersonic jet noise and variation of thrust. The multiple nozzle has same mass flux and nozzle area ratio. When multiple nozzle of eject motor exhausts a plume outside the nozzle, the supersonic blast wave is created and makes a complicated flux. To analyze the complicated flux and to capture the shock, special techniques are required. This study adopts Roe's upwind scheme as a spatial derivative and a second order central scheme for viscous term. The LU-SGS implicit scheme is used for time integration and for an correct prediction; this study used finite-difference solution of the unsteady, compressible, full Navier-Stokes equations, coupled with a two-equation k-ε turbulence model. In addition, the multi-block grid technique is applied to analyze the complicated geometry of the exhaust plume.

INTRODUCTION

Burning propellant, commonly used in a guided missile, accompanies both plume and storm which might make a shooter in a dangerous situation. In specific, burning propellant used in an antitank guided missile accompanies a bigger risk. Furthermore, this antitank guided missile is exposed to higher risk; in particular, when it launches inside, it brings high temperature plume, poisonous gas and big explosion noise. Therefore, it is of importance to protect a shooter from these situations.

Eject motor has been used to address above issues. It is sub propellant equipment which is attached to guided missile's main propellant. When missile is launched, the sub propellant equipment propels the missile from its pad with less propellant fuel. After the missile is far enough (9m) from the shooter, the main motor ignites and flies to the target. As the eject motor is propelled, it separates before it leaves the launching tube and drops a safety way off from the shooter. Though eject motor uses less propellant fuel, it still could be dangerous for a shooter when guided missiles are launched inside.

Multiple nozzles are selected instead of single nozzle because when guided missile is launched inside, there is a possibility that a shooter is not protected and not safe. As discussed in previous research of Ebrahimi [1], the length of the plume is proportional to exit diameter in terms of mass flux and nozzle area ratio. Therefore, multiple nozzles could reduce the plume by decreasing the exit diameter. Also, the noise could be reduced through the interaction of plume, exhausted from multiple nozzles.

Single nozzle could minimize uncertainty of performance as it follows proven design techniques; however, length of the plume gets longer in this case. When length, diameter, weight of the nozzle are limited, because of the long nozzle, the mass center of the rocket will move to the rear and affects guided missile's air dynamics stability. Multiple nozzles, however, improve specific impulse characteristics by decreasing length, weight of the nozzle, and the structure intensity. It also can control scale of the turbulence and dissipation length that concludes to reduce length of the plume and noise. Also, the mass center of rocket moves to the fore part which improves guided missile air dynamics stability. As length decreases, more propellant could be added. Inconsistent structure and materials of multi nozzles with no proven design techniques can be heavier and less efficient than single nozzle. Location of ring-shaped nozzles can cause the plumes interaction which may lead to flux loss and heat loss.

There have been few studies of supersonic flow field from the eject motor with multi nozzles in developed countries. In specific, there were almost no studies about noise-analysis. Hocomb [2] and Ebrahimi [1] studied about the Minuteman

SRMs (solid-propellant rocket motors) with quad nozzles and plume in Titan Rocket Propulsion System with double nozzles by CFD in 1989 and 1997 respectively. The results were, however, mainly about proving the program. The analysis of strong plume interaction by physical state was insignificant. Rhonald [3] analyzed Multi-Jet plume by applying a model in 1996. Also, Chasman [4] studied about optimizing single nozzle and multiple nozzles by optimization techniques in 2004.

Regarding the internal case, studies have been attempted to reduce reaction on impulsive propagation generated at the muzzle and muzzle geometry. However, their studies were not direct one on flux field in Antitank guided missile. In the early 2000, a few studies performed numerical analysis for high pressure blast flow fields of a silencer [5-9].

The main purpose of this study is to compare single nozzle with multiple nozzles to seek for an appropriate theory of multiple nozzles. Multiple nozzles have been compared with single nozzle in terms of characteristics of plume and the change of thrust.

METHOD AND BOUNDARY CONDITIONS OF NUMERICAL ANALYSIS

Method of numerical analysis

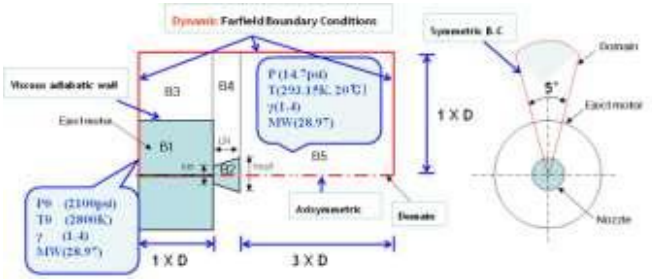

Fig. 1 Computational domain for an eject motor with a single nozzle.

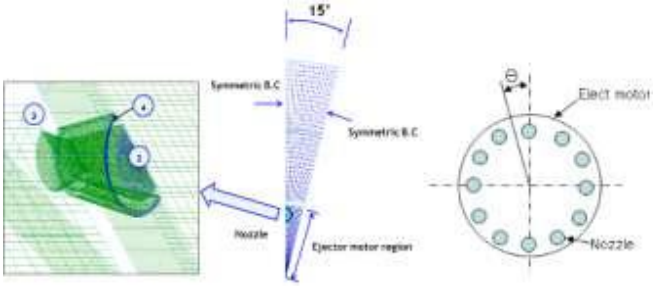

Fig. 2 Computational domain for an eject motor with 12 nozzles.

Table 1 Dimensions and grid points (Single nozzle).

Block	Dimension(J*K*L)	Grid points
I	50×7×50	17,500
II	90×7×30	18,900
III	40×7×60	16,800
IV	25×7×20	3,500
V	300×7×100	210,000
VI	60×7×50	21,000
Total Grid Points		287,700

Table 2 Dimensions and grid points (12 nozzles).

Block	Dimension(J*K*L)	Grid points
I	60×21×50	63,000
II	80×31×50	124,000
III	30×15×30	13,500
IV	30×16×30	14,400
V	400×31×60	744,000
VI	150×21×100	315,000
Total Grid Points		1,273,900

When eject motor exhausts a plume outside the nozzle, blast wave is created and makes a complicated flux. To analyze a complicated flux and to capture the shock, special techniques are required. This study adopts Roe's upwind scheme as a spatial derivative and a second order central scheme for viscous term. The LU-SGS implicit scheme is used for time integration and for an correct prediction; this study used finite-difference solution of the unsteady, compressible, full Navier-Stokes equations, coupled with a two-equation k-ε turbulence model. In addition, the multi-block grid technique is applied to analyze the complicated geometry of the exhaust plume. The grid points in overlapped regions are constructed so as to exactly coincide and to preserve the conservations of fluxes across the grids.

Initially, the internal portion of the eject motor was filled with gases of high pressure and high temperature. The shock wave is located at the nozzle exit. The viscous (no-slip) adiabatic wall boundary condition is applied. At inflow and outflow boundaries, a characteristic boundary condition is applied, which is based on the Riemann invariants.

Boundary conditions of single nozzle analysis

Figure 1 shows the boundary conditions and the computation domain of single nozzle. As the right picture at Figure 1, single nozzle uses the axisymmetric boundary condition on 5°. At inflow and outflow boundaries, a characteristic boundary condition is applied, which is based on the Riemann invariants. When supersonic flow and subsonic flow is coincide. the condition is used. The inlet condition uses total temperature and total pressure inflow condition. The pressure is 2100 psi and the temperature is 2800 K. 281000 grid points have been used as Table 1 and 42.4 hours have been used to analyze the flow domain 3D (0.3m).

Figure 2 shows the boundary conditions and the computation domain of multiple nozzles. It has 12 nozzles and its computation domain is 15°. As the center of picture provides, symmetric boundary conditions are applied on both sides. As the left picture provides, the nozzle uses overset grid and are composed by 3 blocks. Block 2 is the inside flow domain of the nozzle, Block 3 is the outside domain, and Block 4 is between Block 2 and 3 which wraps the outside of the nozzle. Also, when block 3 is analyzed, it performs hole-cutting at DCF3D. Approximately 1.2 million grid points is used to well express the shock wave near the outlet of the nozzle.

RESULTS OF ANALYSIS

Figs. 3, 6, and 8 show the Mach number contour on each time of the single nozzle. As Figs. 4, 7 and 9 show, the active transference at the boundary layer is confirmed. Temperature

increases after the shock wave at the middle axis of the nozzle. Figure 5 shows the pressure contour and precursor shock occurred on the front of the fluid process.

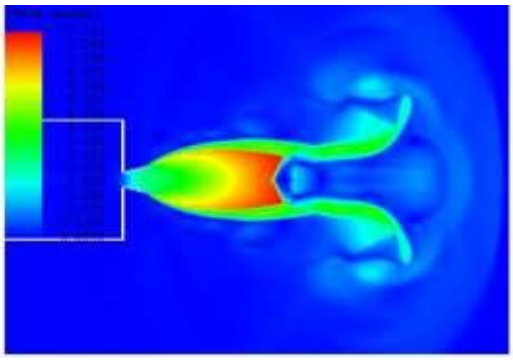

Fig. 3 Mach number contour of single nozzle, t=0.53ms.

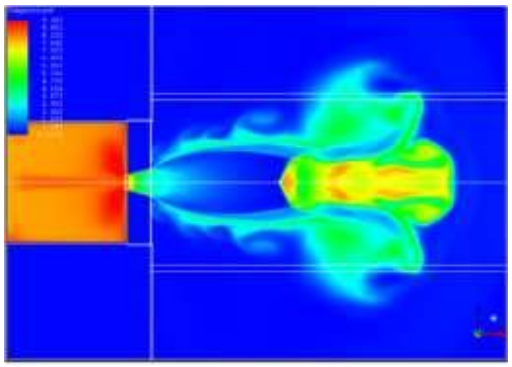

Fig. 4 Temperature contour of single nozzle, t=0.53ms.

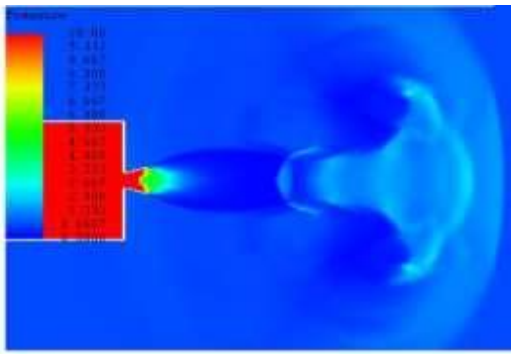

Fig. 5 Pressure contour of single nozzle, t=0.53ms.

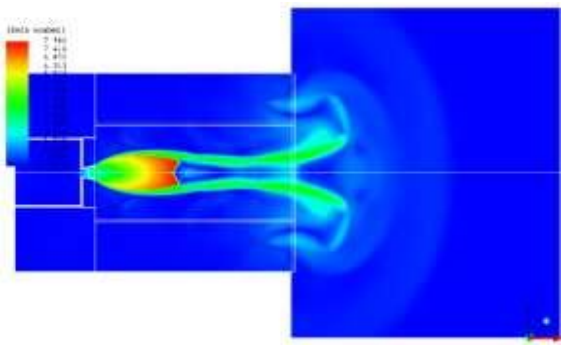

Fig. 6 Mach number contour of single nozzle, t=1.05ms.

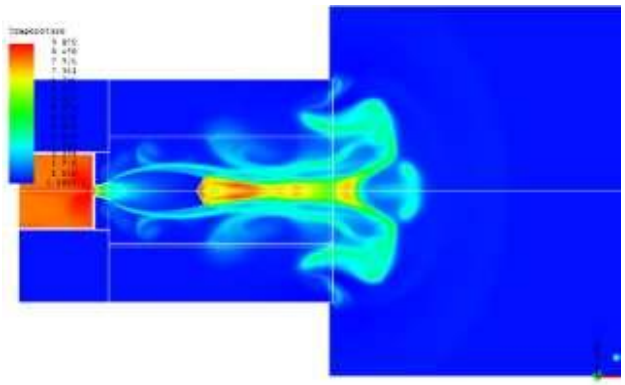

Fig. 7 Temperature contour of single nozzle, t=1.05ms.

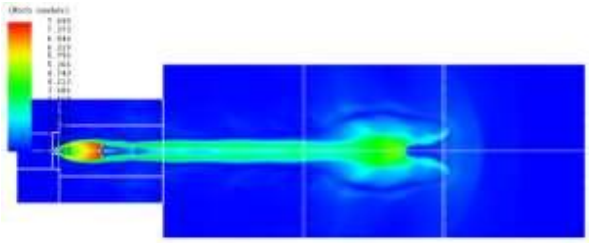

Fig. 8 Mach number contour of single nozzle, t=3.16ms.

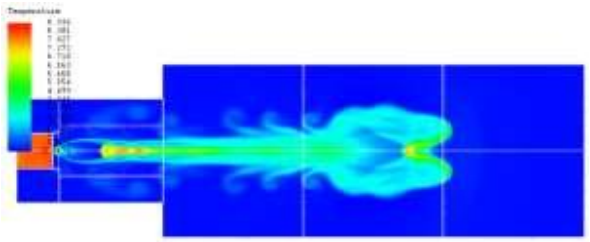

Fig. 9 Temperature contour of single nozzle, t=3.16ms.

Figure 10 and 11 show the single nozzle variation of temperature depending on time. Fig. 10 shows the near region on the nozzle exit. The nozzle exit region point is X/D=0. The X-axis X/D is the distance from the nozzle exit and the Y-axis is the temperature [K]. As it passes the nozzle from the eject motor, the temperature decrease until X/D=1, and after the shock occurs at X/D=1.0, the temperature increases the same as the temperature of the eject motor. Temperature keeps increasing until it is affected by the flow and starts decreasing to the atmosphere temperature.

Figure 11 shows the comparison of the temperature contour at far region on the nozzle exit. When X/D=1.0, the temperature increases sharply as in Fig. 10 and starts decreasing. However, the temperature is still high and follows the flow course depending on time in front of the flow process.

Figure 12 and 15 show Mach number distribution about the multiple nozzles. It is shown that the exhausted plume is being mixed in the middle of the eject motor on the top and bottom of Y-plane of the multiple nozzles. Through this interaction, Figure 13 and Figure 16 show the temperature is increasing on the center line of the multiple nozzles depending on the time. Figure 14 and Figure 17 show the pressure distribution and the pressure are both increasing through the interaction.

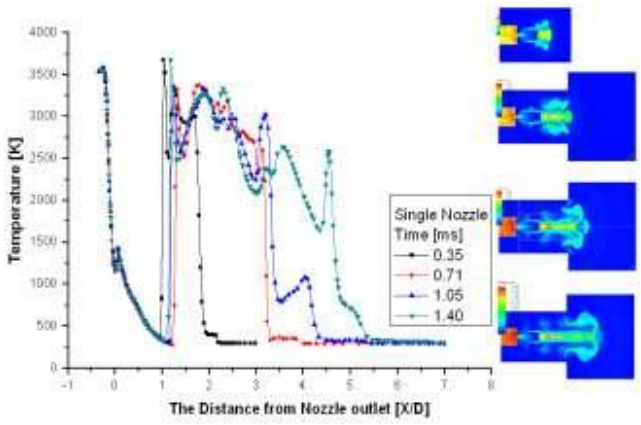

Fig. 10 Variations of temperature depending on the time, near region on the nozzle exit.

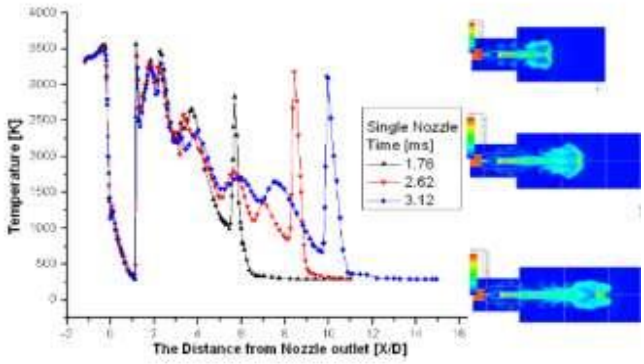

Fig. 11 Variations of temperature depending on the time, far region on the nozzle exit.

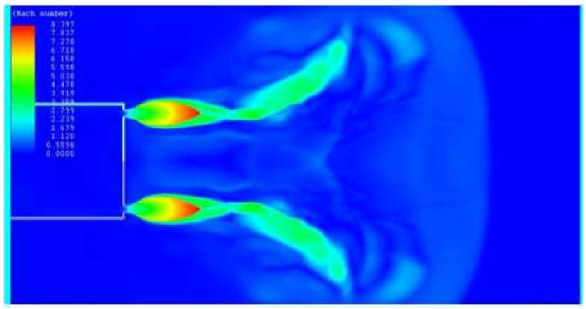

Fig. 12 Mach number contour of multi-nozzle, t=0.53ms.

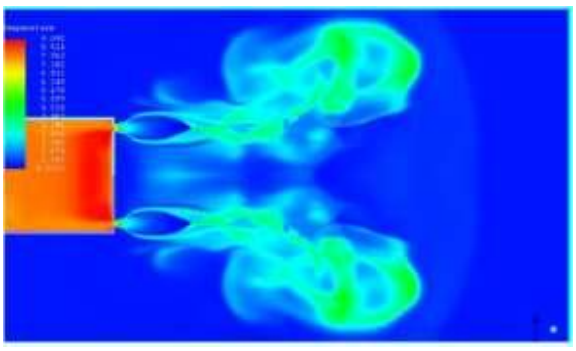

Fig. 13 Temperature contour of multi-nozzle, t=0.53ms.

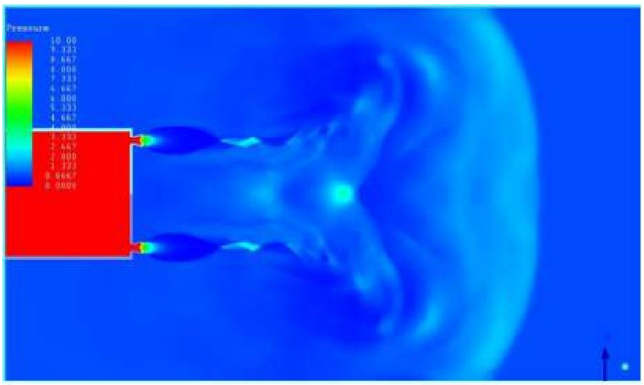

Fig. 14 Pressure contour of multi-nozzle, t=0.53ms.

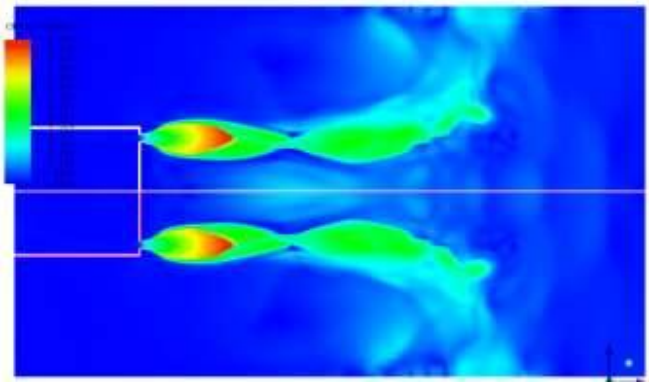

Fig. 15 Mach number contour of multi-nozzle, t=0.87ms.

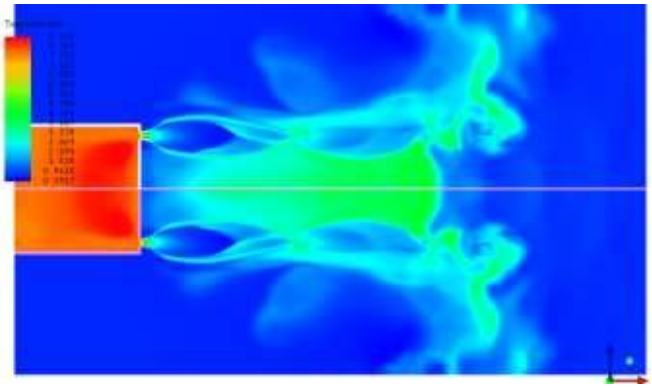

Fig. 16 Temperature contour of multi-nozzle, t=0.87ms.

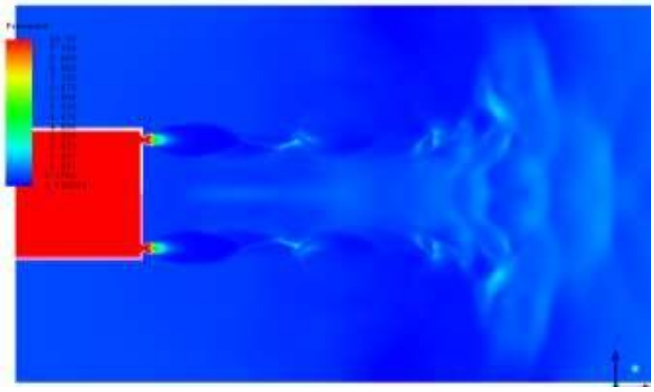

Fig. 17 Pressure contour of multi-nozzle, t=0.87ms.

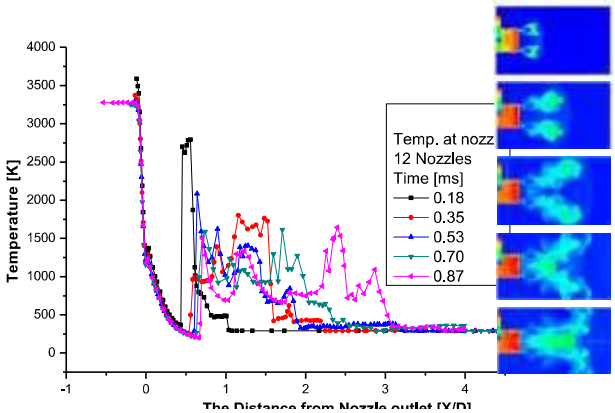

Fig. 18 Variations of temperature depending on the time (Multi-nozzle, center line of nozzle)

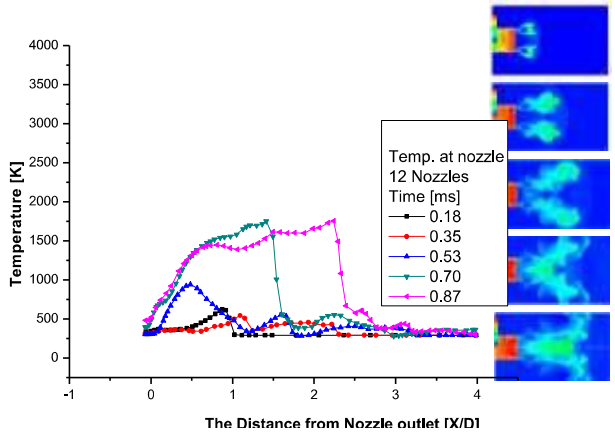

Fig. 19 Variations of temperature depending on the time (Multi-nozzle, center line of eject motor)

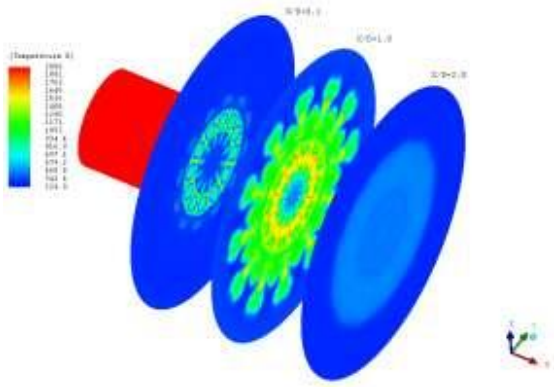

Fig. 20 Temperature contours on X-plane, t=0.35ms.

Figure 18 shows the variation of temperature depending on the time on the center line of the multiple nozzles. As it passes the nozzle from the eject motor, the temperature decreases until X/D=0.5 and after the shock occurs at X/D=0.5, the temperature increases even though the time pass and the location are the same and at this part the increased temperature starts decreasing as it gets far from the nozzle. Figure 19 shows variation of temperature depending on the time on the center line of the eject motor. After 0.70 ms, the temperature is the same as 1500 [K]; the temperature graph shows that the X/D is almost equivalent to that of in the low values. This graph is shown that once it is formed in a fixed form, it almost does't change.

Figure 20 and Figure 22 show the temperature distribution contours on the X-plane. They show the comparison of the temperature distribution from the nozzle. The exhausted plume from 12 nozzles are moving to the center line on the eject motor. High temperature is formed in the center of the eject motor. Figure 21 and Figure 23 show the Mach number contours on the X-plane. They also show the exhausted plume being mixed.

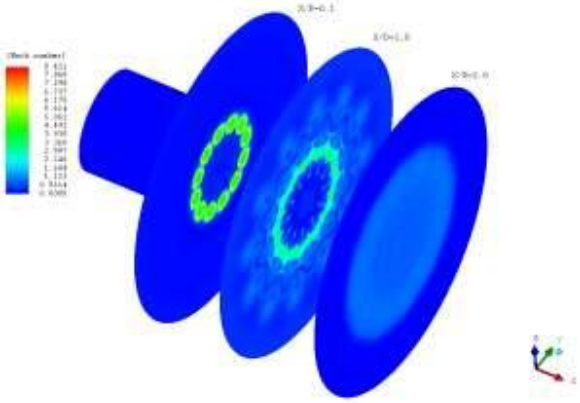

Fig. 21 Mach number contours on X-plane, t=0.35ms.

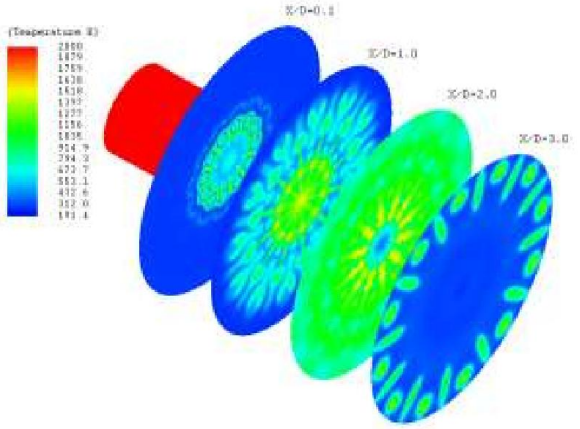

Fig. 22 Temperature contours on X-plane, t=0.70ms.

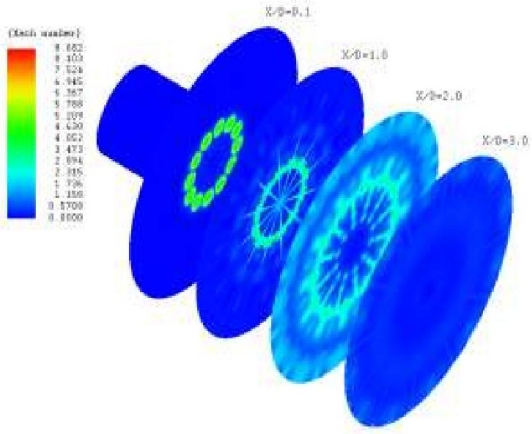

Fig. 23 Mach number contours on X-plane, t=0.70ms.

Figure 24 shows the graph of Mach numbers at 0.53 ms which has compared the single nozzle with the multiple nozzles. The temperature of the single nozzle decreases sharply at X/D=1.0 and the temperature of the multiple nozzles is decreasing as 0.5. In the case of multiple nozzles, temperature drop stops on a higher temperature than it does on the single nozzle. Then it repeats up and down. After the temperature drops again at X/D=1.5, it approaches to the atmosphere temperature. As it is shown at the right figure, the single nozzle boundary layer doesn't intersect after the shock has occurred. However, the multiple nozzles proceeds after they mix up and bring the result as the graph. Figure 25 shows the variation of the temperature depending on the time (comparison of single and multiple nozzles). The single nozzle has a higher temperature and has a wider distribution as well. Also, the temperature of the multiple nozzles gets closer to the atmosphere temperature at a closer distance than the single nozzle. Figure 26 shows the pressure depending on the distance from the nozzle exit of two cases. As the high pressure passes through the nozzle, the pressure decreases sharply. After passing shock, it increases weakly but decreases again.

Based on these results, it is found that multiple nozzles have lower pressure distribution than the single nozzle. However, the pressure distribution of the eject motor with multiple nozzles on the center line has a high pressure section.

CONCLUSIONS

This study performed unsteady analysis regarding 3 dimension exhaust plume and comparison of two cases of each characteristic. Flow characteristic in transition region was proved by the use of computational domain analysis from the near field to the far field. In case of the single nozzle, the first mach disk was formed near X/D = 1.0; the mach disk was formed near X/D = 0.5. in multiple nozzles. The temperature near the Eject motor's center increases in process of time because of the interaction of plumes exhausted from multiple nozzles. In conclusion, the plume length is predicted to reduce risk.

ACKNOWLEDGMENTS

This research has been supported by the Agency for Defense Development.

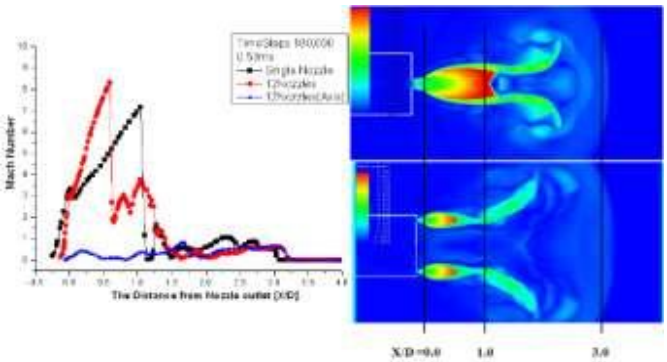

Fig. 24 Variations of Mach number depending on the time.

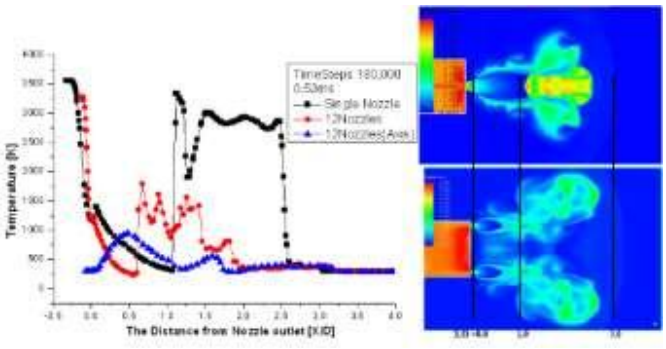

Fig. 25 Variations of temperature depending on the time.

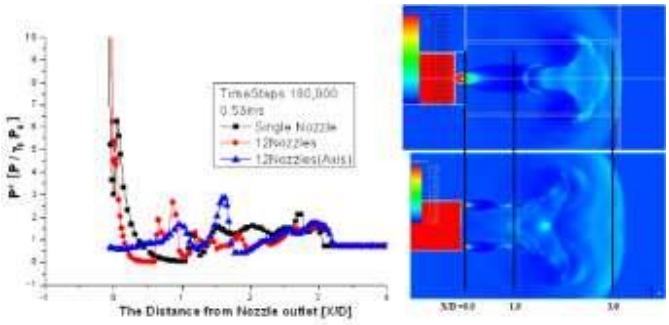

Fig. 26 Variations of pressure depending on the time.

REFERENCES

[1] Ebrahimi, "Numerical Investigation of Multi-Plume Rocket Phenomenology," AIAA97-2942, 1997.

[2] Hocomb, "Three-Dimensional Navier-Stokes Rocket Plume Calculations," AIAA89-1986-CP , 1989.

[3] Rhonald M. Jenkins, Winfred A. Foster Jr. and Lora S. Wirth, "Numerical analysis of unsteady multiple jet plume interactions," *Applied Mathematics and Computation*, Vol. 79, Issues 2-3, 1996, pp. 239-247.

[4] D. Chasman, M. Birch, S. Haight, M. Osborne, Y. Oh and A. Hink, "Multi-Disciplinary Optimization Method for an Innovative Multi Nozzle (MNG) Design," AIAA-2004-619-690, 2004.

[5] Ko, S. H., Woo, S. D. and Kang, K. J., "Numerical Analysis for a Simple Shape Silencer for Intensity Diminution of High Pressure Blast Flow Fields," *Korean Society of Computational Fluids Engineering Autumn Conference*, 2004, pp. 91-94.

[6] Lee, D. J., Lee, I. C., Woo, S. D., Kang, K. J. and Kim, I. W., "Study on Blast Noise in Supersonic Flow," *The 2005 Congress and Exposition on Noise Control Engineering*, *Inter-Noise*, 2005.

[7] S. H. Ko, D. S. Lee, S. D. Woo and K. J. Kang, "Numerical Analysis for a Silencer of Tank Gun," *Korean Society of Computational Fluids Engineering*, Vol. 10, No. 4, 2005, pp. 59-65.

[8] D. S. Lee, S. H. Ko and K. J. Kang, "Numerical Analysis for High Pressure Blast Flow Fields of a Silencer with Baffles," *Korean Society of Computational Fluids Engineering Autumn Conference*, 2005, pp. 169-172.

[9] D. S. Lee, S. H. Ko and K. J. Kang, "A Numerical Analysis for The Baffled Silencer for the Noise Diminution of Tank Gun," *Trans. of the KSME B*, Vol. 31, No. 3, 2007, pp. 217-224.